

Metal-Based Turn-On Fluorescent Probes for Sensing Nitric Oxide

MI HEE LIM AND STEPHEN J. LIPPARD*

Department of Chemistry, Massachusetts Institute of Technology, Cambridge, Massachusetts 02139

Received June 1, 2006

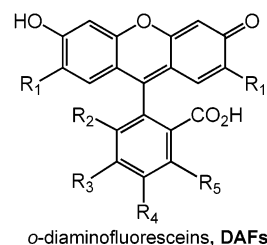
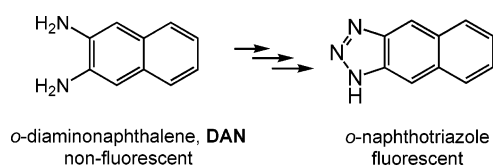
ABSTRACT

Nitric oxide, a reactive free radical, regulates a variety of biological processes. The absence of tools to detect NO directly, rapidly, specifically, and selectively motivated us to synthesize metal-based fluorescent probes to visualize the presence of NO. We prepared and investigated Co(II), Fe(II), Ru(II), Rh(II), and Cu(II) complexes as turn-on fluorescent NO sensors. Our exploration has provided insight into how the interaction of transition-metal centers with nitric oxide can be utilized for NO sensing.

Introduction

Nitric oxide (NO) is produced by inducible and constitutive nitric oxide synthases (iNOS and cNOS), resulting in a wide range of concentrations in biological systems.^{1–3} Depending on its concentration and location, NO can have diverse biological functions. At low concentrations, NO regulates vasodilation in the circulatory system and long-term potentiation in the brain.^{1–3} In contrast, micromolar concentrations of NO can trigger the formation of reactive nitrogen species (RNS), leading to carcinogenesis and neurodegenerative disorders but also providing a defense against invading pathogens.^{2,3}

Since NO is a free radical that rapidly diffuses through most cells and tissues and reacts with biological targets,^{4,5} its formation and migration are not easily monitored in biology. Fluorescence detection allows imaging of intracellular and extracellular NO when combined with microscopy, providing high spatiotemporal resolution^{6,7} compared to other methods such as chemiluminescence,⁸ EPR spectroscopy,⁶ and amperometry.⁹ For bioimaging of NO, the commercially available organic molecule-based sensors *o*-diaminonaphthalene (DAN) and *o*-diaminofluoresceins (DAFs) (Figure 1) are commonly used.^{6,7} Their fluorescent response, however, requires formation of a triazole species by oxidized NO products such as N₂O₃. They are therefore unable to monitor NO itself, which



DAFs	R ₁	R ₂	R ₃	R ₄	R ₅
DAF-1	H	H	H	NH ₂	NH ₂
DAF-2	H	H	NH ₂	NH ₂	H
DAF-3	H	NH ₂	NH ₂	H	H
DAF-4	Cl	H	H	NH ₂	NH ₂
DAF-5	Cl	H	NH ₂	NH ₂	H
DAF-6	Cl	NH ₂	NH ₂	H	H

FIGURE 1. Chemical structures of DAN and DAFs.

means that NO-related bioevents would not be detected in real time.

There are several requirements for fluorescent nitric oxide sensors to be useful in biology. Probes should be nontoxic and afford direct, fast, reversible, specific, and selective NO detection. It is preferable that they contain fluorophores that excite and emit in the visible or near-infrared region in order to avoid interference or cellular damage by UV light. Real-time imaging with spatial resolution is desirable.

To address the lack of suitable NO sensors, we explored the reactions between nitric oxide and transition-metal complexes to devise metal-based fluorescent sensors that satisfy the aforementioned criteria. This Account describes the evolution of transition-metal-based strategies for nitric oxide sensing as well as detailed mechanistic studies of the underlying chemistry by our research group and others.

Strategies for Metal-Based Fluorescent Nitric Oxide Sensing

The first metal-based fluorescent nitric oxide sensor, an iron cyclam complex, exhibited diminished emission intensity upon NO binding to the iron center.^{7,10} An iron dithiocarbamate complex with an acridine–TEMPO ligand also displayed a decrease in fluorescence after NO binding.^{7,11} Fluorescence enhancement is generally preferred over fluorescence quenching when monitoring an analyte

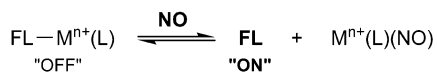
* To whom the correspondence should be addressed. E-mail: lippard@mit.edu.

Mi Hee Lim was born in Kwang Myung-City, Korea, in 1977. She received her B.S. and M.Sc. degrees in Chemistry under the direction of Professor Wonwoo Nam from Ewha Womans University, Seoul, Korea. She received her Ph.D. degree in Inorganic Chemistry under the supervision of Professor Stephen J. Lippard in the Department of Chemistry at the Massachusetts Institute of Technology in 2006. Her research interests include metal-based fluorescent sensors for nitric oxide.

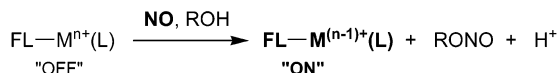
Stephen J. Lippard is the Arthur Amos Noyes Professor of chemistry at M.I.T., where he was Head of the Chemistry Department from 1995 to 2005. His research activities span the fields of inorganic chemistry, biological chemistry, and metalloneurochemistry.

Scheme 1. Strategies for Metal-Based NO Sensing

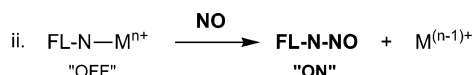
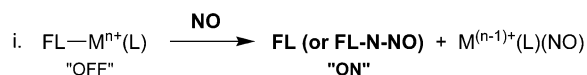
(a) Fluorophore Displacement without Metal Reduction



(b) Metal Reduction without Fluorophore Displacement



(c) Metal Reduction with Fluorophore Displacement



in biological systems. When we embarked on our research, no examples of metal-based turn-on fluorescent nitric oxide sensors existed. Our approach to achieving this objective and detection of NO production in living cells with the use of one such probe form the basis of the present Account.

Fluorophore Displacement without Metal Reduction.

This approach relies upon formation of a metal–nitrosyl adduct, releasing a fluorophore that was initially quenched by coordination to a paramagnetic transition-metal center by electron or energy transfer (Scheme 1.a).¹² Fluorophores can bind the metal center as axial ligands. Introduction of nitric oxide causes their displacement with concomitant fluorescence turn on. This strategy has been applied for an iron cyclam complex,⁷ ruthenium porphyrins,¹³ and dirhodium tetracarboxylate complexes.^{7,14}

Metal Reduction without Fluorophore Displacement.

Nitric oxide can reduce Cu(II) to Cu(I) in the presence of methanol or water (ROH), forming RONO and H⁺ (R = Me or H), without loss of a fluorescent ligand from the coordination sphere (Scheme 1.b).¹⁵ Detailed mechanistic studies of such reactions suggested to us that Cu(II)-based nitric oxide chemistry might form the basis for a sensing strategy.¹⁵ In particular, fluorophore fluorescence, quenched in a paramagnetic Cu(II) environment, might be restored upon NO-induced reduction to a diamagnetic Cu(I) species with retention of the fluorophore ligand (Scheme 1.b). We devised three Cu(II) systems to explore this approach.^{16,17}

Metal Reduction with Fluorophore Displacement.

Reductive nitrosylation can accompany the reactions of NO with complexes of redox-active metal ions, including Co(II) and Fe(III), where the nitrosated ligand is displaced.^{15,18} In this reaction a fluorescent ligand initially coordinated to the metal ion is dissociated with concomitant fluorescence turn on following exposure to NO. Such displacement of a ligand fluorophore by NO was a key feature of our first fluorescent NO sensors, cobalt–DATI (DATI = dansyl-aminotroponimine, Figure 2) and cobalt(II) tetracarboxylate compounds (Scheme 1.c.i).^{18,19}

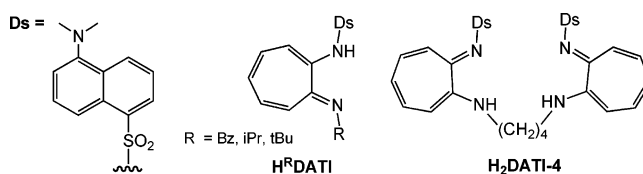


FIGURE 2. Chemical structures of H^RDATI and H₂DATI-4.

During metal reduction by NO, a species with NO⁺ character can react with an amine functionality to produce an *N*-nitrosamine.²⁰ If the fluorophore contains a coordinated amine, it can become *N*-nitrosated by an intramolecular pathway with concomitant dissociation and fluorescence enhancement (Scheme 1.c.ii). Such increased fluorescence was observed in the reaction of a copper anthracenyl-cyclam complex with NO to form an *N*-nitrosated cyclam ligand.²¹ Utilizing this fluorophore-displacement *N*-nitrosation strategy, metal-based sensors for detecting NO were developed. We constructed a copper(II) fluorescein complex for NO sensing based on this approach.²²

Cobalt(II) Complexes²³

Co–DATI Systems. The reactions of cobalt(II) tropocoronand complexes with NO were previously investigated in our laboratory.²⁴ This NO chemistry suggested that Co(II) H^RDATI and H₂DATI-4 systems (Figure 2) might be suitable targets for fluorescent NO sensor development. We prepared four Co(II) complexes [Co(^{iPr}DATI)₂] (**1**), [Co(^{tBu}DATI)₂] (**2**), [Co(^{Bz}DATI)₂] (**3**), and [Co(DATI-4)] (**4**) (Figure 3)¹⁸ having pseudo-tetrahedral geometries with dihedral angles between the 5-membered chelate rings of 76.1°, 81.4°, 73.8°, and 62.2°, respectively.¹⁸ These values reflect the different steric requirements of the R substituents. The dansyl groups in **3** and **4** align in a parallel-planar fashion with an average distance between the ring planes of 3.5(1) and 3.63(9) Å, respectively. These distances are within range for π–π stacking interactions,²⁵ which could possibly contribute to the quenching of the dansyl group fluorescence.

The fluorescence of a 40 μM solution of **1** in CH₂Cl₂ is only 5–6% of the intensity of the free ligand (Figure 4).¹⁸ This fluorescence quenching is hypothesized to result mainly from interactions between the excited fluorophore and the cobalt(II) d-orbital manifold by electron or energy transfer.¹² Upon addition of NO to the solution, a steady 8-fold fluorescence increase relative to that of the starting complex **1** was noted over 6 h (Figure 4).¹⁸ The initial fluorescent response of **4** to NO is faster than that of **1**, however. A 2-fold fluorescence increase occurred within 3 min in CH₂Cl₂, and the emission continued to rise over 6 h to a final 4-fold enhancement.¹⁸ The lower limit of NO detection by **4** is 50–100 μM.¹⁸ The tetramethylene linker chain in **4** (Figure 3) distorts the Co(II) geometry relative to that in **1**, **2**, and **3**, which may cause its differential NO reactivity.

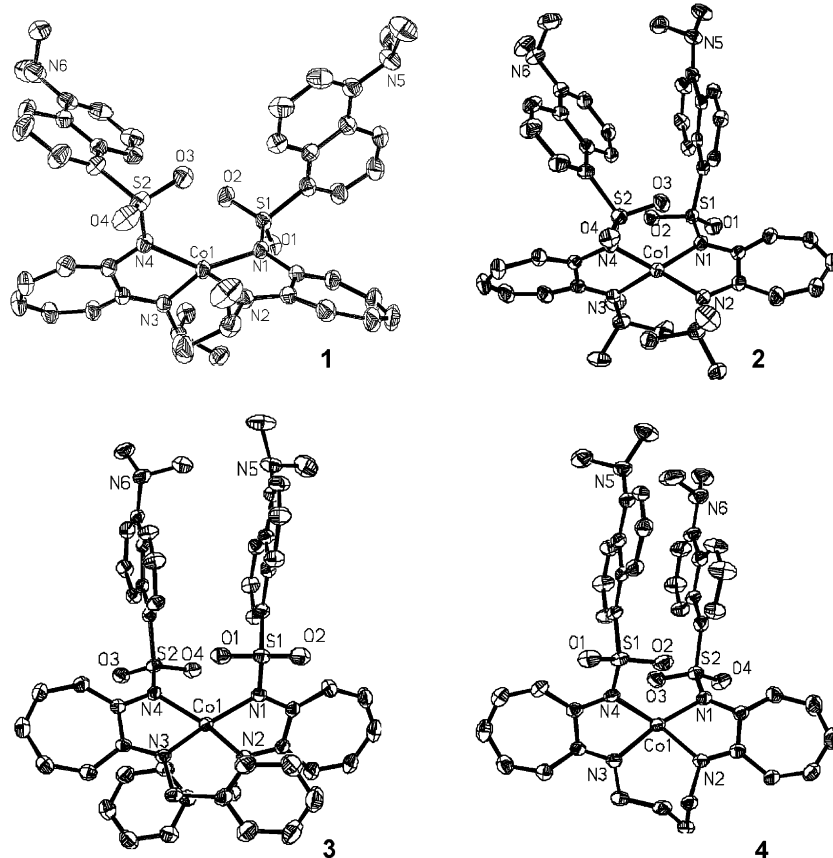


FIGURE 3. ORTEP diagrams of **1–4** showing 50% probability thermal ellipsoids. Reprinted with permission from ref 18. Copyright 2000 American Chemical Society.

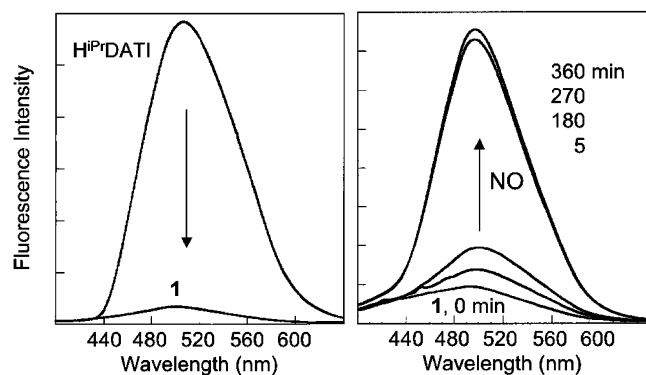
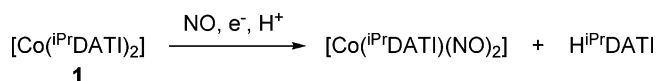


FIGURE 4. Fluorescence response of **1** compared to $\text{H}^{\text{iPrDATI}}$ (right) and of **1** upon addition of excess NO (left), excited at 350 nm. Adapted with permission from ref 18.

The NO-induced fluorescence enhancement in these reactions is a consequence of fluorophore dissociation, which accompanies formation of Co(I)–dinitrosyl adducts as revealed by IR and ^1H NMR spectroscopy. Several hours after addition of excess NO to CH_2Cl_2 solutions of **1**, two IR bands appeared at 1838 and 1760 cm^{-1} , indicating the presence of dinitrosyl complexes.¹⁸ The ^1H NMR spectrum after the reaction revealed two sets of resonances for diamagnetic compounds corresponding to the free ligand $\text{H}^{\text{iPrDATI}}$ and the $\{\text{Co}(\text{NO})_2\}^{10}$ species $[\text{Co}(\text{NO})_2(\text{iPrDATI})]$.¹⁸ Thus, the chemistry proceeds by a reductive nitrosylation mechanism (Scheme 2) with turn-on emission arising

Scheme 2. NO Reactivity of Co–DATI Complexes



from fluorophore dissociation upon NO binding to Co(II) (Scheme 1.c.i).

Dicobalt(II) Tetracarboxylate Chemistry. A dicobalt(II) tetracarboxylate complex with *N*-donor ligands, $[\text{Co}_2(\mu\text{-O}_2\text{CAR}^{\text{Tot}})_2(\text{O}_2\text{CAR}^{\text{Tot}})_2(\text{py})_2]$, where $\text{O}_2\text{CAR}^{\text{Tot}} = 2,6\text{-di}(p\text{-tolyl})\text{benzoate}$ and $\text{py} = \text{pyridine}$, was previously reported by our laboratory.²⁶ The properties of this complex, including its air stability and binding of an *N*-donor ligand to the metal core, inspired us to prepare derivatives having appended fluorophore-modified nitrogen bases as potential fluorescent NO sensors. The dicobalt(II) complex of dansyl-piperazine (Ds-pip) was synthesized and found to exist in solution as an equilibrium mixture of windmill $[\text{Co}_2(\mu\text{-O}_2\text{CAR}^{\text{Tot}})_2(\text{O}_2\text{CAR}^{\text{Tot}})_2(\text{Ds-pip})_2]$ (**5**) and paddlewheel $[\text{Co}_2(\mu\text{-O}_2\text{CAR}^{\text{Tot}})_4(\text{Ds-pip})_2]$ (**6**) geometric isomers, depending on the temperature (Figure 5).¹⁹ Compound **6** is the predominant species in solution at room temperature.

When a CH_2Cl_2 solution of **6** ($100\ \mu\text{M}$) was allowed to react with 150 equiv of NO, a 9.6-fold fluorescence increase occurred within 1 h and the emission maximum shifted from 503 to 513 nm ($\lambda_{\text{ex}} = 350\text{ nm}$).¹⁹ IR spectroscopy in situ revealed two prominent bands at 1864 and 1783 cm^{-1} , consistent with formation of a Co(I) dinitrosyl adduct. A band at 1610 cm^{-1} in **6** attributed to a carbox-

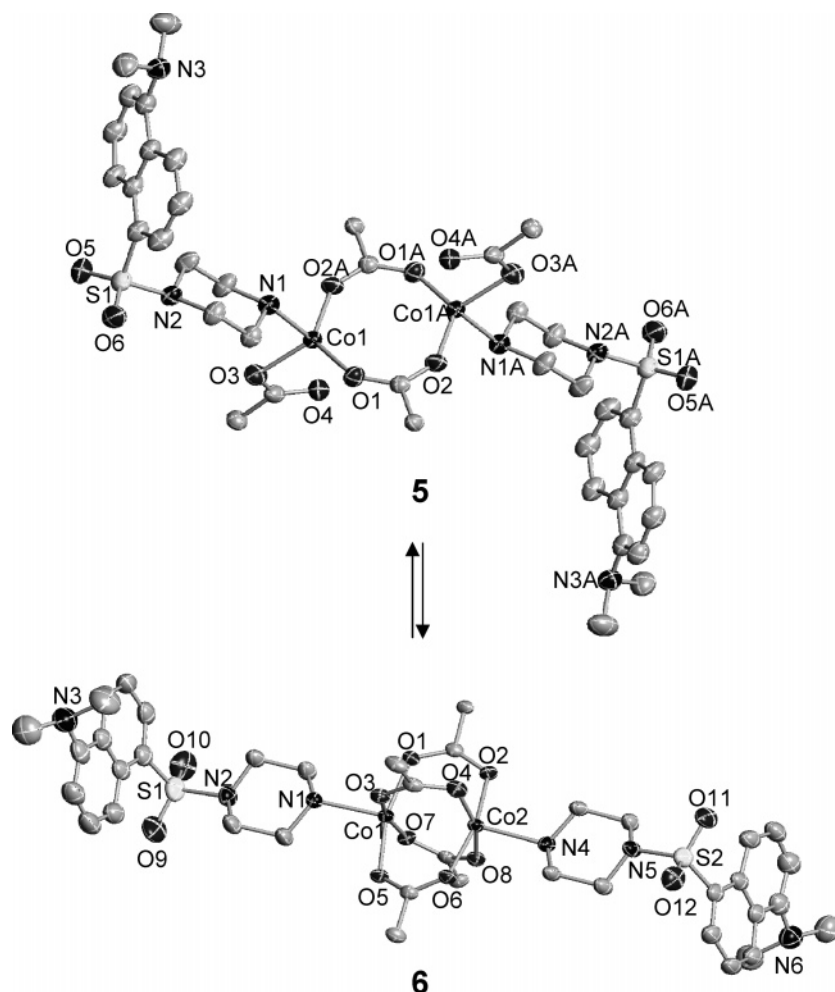


FIGURE 5. ORTEP diagrams of windmill **5** and paddlewheel **6** showing 50% probability thermal ellipsoids. The phenyl rings of $\text{Ar}^{\text{ToI}}\text{CO}_2^-$ ligands have been omitted for clarity. Adapted with permission from ref 21. Copyright 2004 American Chemical Society.

ylate C=O stretching mode disappeared during the NO reaction and was replaced by a new band at 1745 cm^{-1} , assigned to the free carboxylic acid. These results indicate a structural change at the metal center involving the carboxylate ligands.¹⁹ X-ray crystallographic analysis revealed formation of the dicobalt tetranitrosyl complex $[\text{Co}_2(\mu\text{-O}_2\text{CAR}^{\text{ToI}})_2(\text{NO})_4]$ and *N*-nitroso dansyl-piperazine during the reaction. Thus, NO reductively nitrosylates **6** at the dicobalt(II) core, generating a species with NO^+ character, which in turn nitrosates the ligand with concomitant dissociation from cobalt and turn-on fluorescence emission (Scheme 3). The observed formation of the *N*-nitrosated fluorophore ligand helps to explain the shift in emission maximum after the NO reaction.¹⁹ Thus, the fluorophore dissociation strategy (Scheme 1.c.i), involving *N*-nitrosation of the fluorophore ligand during reductive nitrosylation at the metal center, is responsible for the increase of fluorescence upon treatment of these dicobalt systems with NO.

Other Cobalt Dansyl Complexes. To improve the solubility as well as the kinetics of fluorescence turn on by NO in the Co(II) systems, we synthesized the nonfluorescent air-stable Co(II) complexes $[\text{Co}(\text{Ds-AMP})_2]$ (**7**) and $[\text{Co}(\text{Ds-AQ})_2]$ (**8**), where Ds-AMP and Ds-AQ are the conjugate bases of dansyl-aminomethylpyridine (Ds-

HAMP) and dansyl-aminoquinoline (Ds-HAQ).²⁷ X-ray crystallographic determinations of both complexes revealed a pseudo-tetrahedral geometry similar to that of the Co-DATI complexes (Figure 6).

Fluorescence enhancement of **7** and **8** upon NO treatment occurred in both CH_3CN (dielectric constant 37.5) and CH_3OH (32.6) solvents, which are closer in polarity to water (80.2) than CH_2Cl_2 (9.1). Upon admission of NO to CH_3CN solutions of Co(II) complexes (10 μM), the fluorescence increased by 2.1-fold within 35 min for **7** and by 3.6-fold within 20 min for **8**, restoring one-half of that displayed by 2 equiv of the free ligands, Ds-HAMP or Ds-HAQ ($\lambda_{\text{ex}} = 342\text{ nm}$).²⁷ As in the reaction of Co-DATI complexes with NO (Scheme 2),¹⁸ a diamagnetic dinitrosyl adduct and one free ligand were formed in the reaction of **7** with NO, as confirmed by IR ($\{\text{Co}(\text{NO})_2\}$, $\nu_{\text{NO}} = 1766$ and 1693 cm^{-1}) and ^1H NMR (two sets of diamagnetically shifted peaks) spectroscopy. Thus, NO sensing by turn-on fluorescence using **7** and **8** occurs by ejection of one fluorophore ligand from the cobalt coordination sphere via reductive nitrosylation (Scheme 1.c.i).

Co-FATI Systems. The dansyl group is not optimal for *in vivo* imaging of NO because it requires high excitation energy, which can damage cells. We therefore designed two Co(II) complexes with fluorescein-based ligands

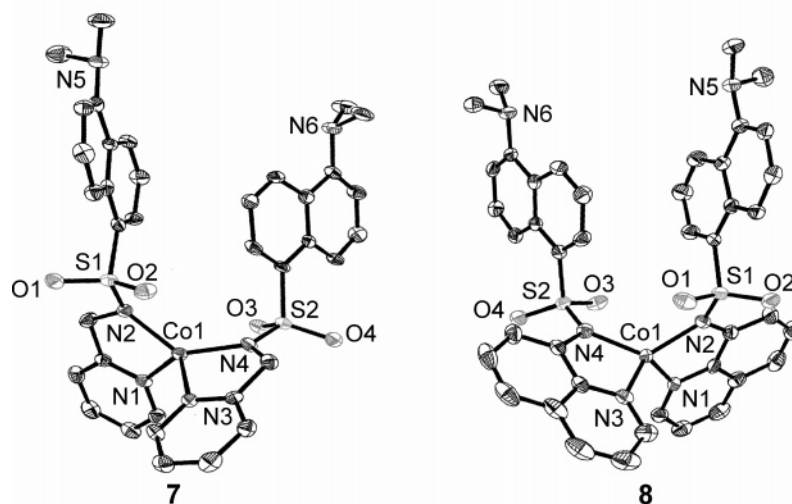
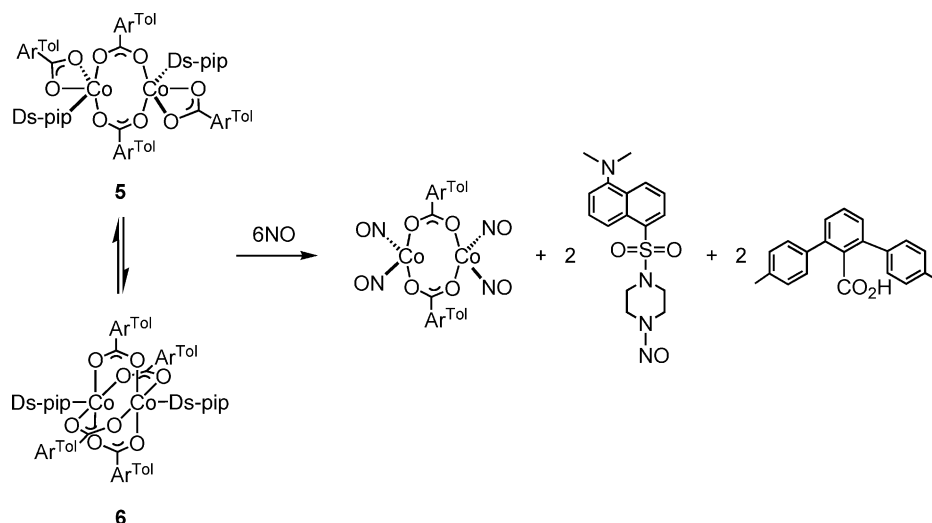


FIGURE 6. ORTEP diagrams of **7** and **8** showing 50% probability thermal ellipsoids. Reprinted with permission from ref 27. Copyright 2006 Wiley-VCH Verlag GmbH & Co. KGaA, Weinheim.

Scheme 3. NO Reactivity of **5** and **6**



[Co(^{iPr}FATI-3)] (**9**) and [Co(^{iPr}FATI-4)] (**10**) (Figure 7).²⁸ Although X-ray structure determinations of **9** and **10** were not obtained, both complexes are likely to be mononuclear based on mass spectrometric analyses. Compound **10** might have a dinuclear structure by analogy to that of the related complex [Co₂(^{iPr}SATI-4)₂] (SATI = salicylaldimine) (Figure 8), however.²⁸

Addition of NO to CH₃OH solutions of **9** and **10** (10 μM) showed a fluorescence increase of only 20% over 4 h for **9** and 3-fold over 22 h for **10** (λ_{ex} = 503 nm, λ_{em} = 530

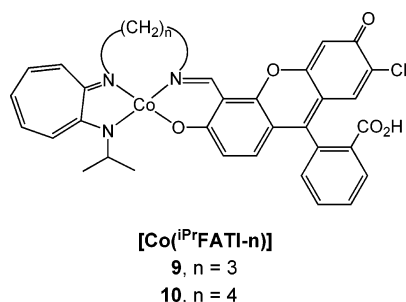


FIGURE 7. Chemical structures of **9** and **10**.

nm), which is significantly slower than encountered with the previous Co(II) systems.^{18,19,27,28} Infrared studies of the reaction of **9** with NO indicate the presence of mononitrosyl (1630 cm⁻¹) and dinitrogen (2114 cm⁻¹) adducts.²⁸ We cannot rule out formation of dinitrosyl species, however, since an intense band for the fluorescein carboxylic acid at 1759 cm⁻¹ overlaps the IR bands of ν_{NO} in {Co(NO)₂}. Complex **10** also formed the 2117 cm⁻¹ band, which most likely corresponds to a dinitrogen adduct. Since multiple products are encountered during the reaction, it is not clear from which of these species fluorescence enhancement arises.

Iron(II) Complexes²³

Iron(II) Mmc-cyclam. An Fe(II) methoxycoumarin-pendent cyclam (Mmc-cyclam) scaffold containing a fluorescein-amine-PROXYL group (**11**, Scheme 4) was prepared as a ratiometric fluorescent NO sensor with the aim of utilizing the fluorophore-displacement strategy (Scheme 1.a).^{7,29} When **11** is excited at 360 nm, fluorescence resonance

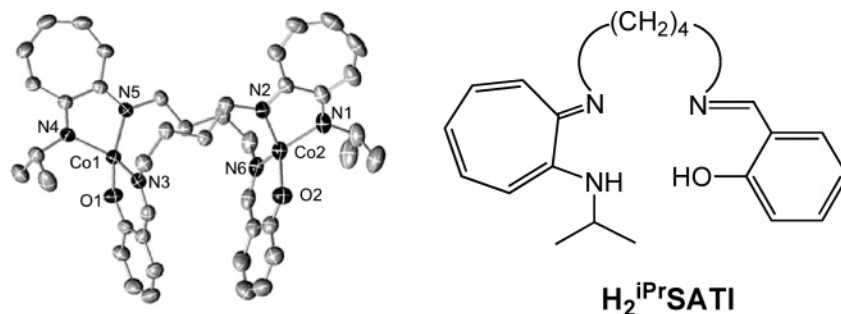
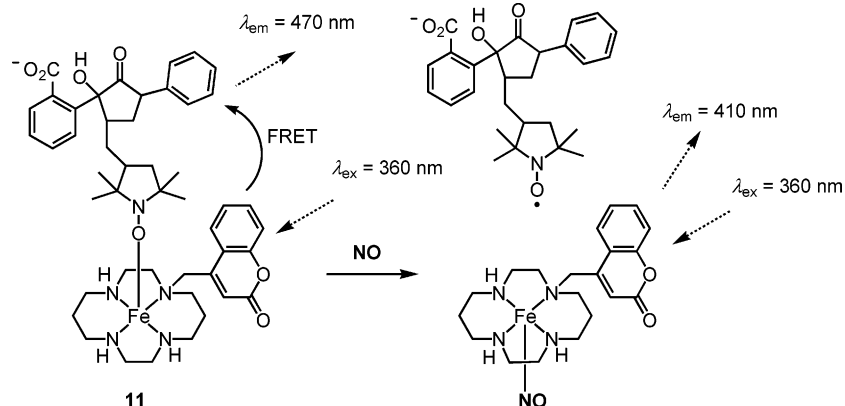


FIGURE 8. ORTEP diagram of $[\text{Co}_2(\text{iPrSATI-4})_2]$ showing 50% probability thermal ellipsoids (left, adapted with permission from ref 28 with permission, Copyright 2004 American Chemical Society) and a chemical structure of $\text{H}_2\text{iPrSATI}$ (right).

Scheme 4. NO Detection by 11



energy transfer (FRET) occurs from Mmc-cyclam ($\lambda_{\text{ex}} = 360 \text{ nm}$, $\lambda_{\text{em}} = 410 \text{ nm}$) to fluorescamine-PROXYL ($\lambda_{\text{ex}} = 360 \text{ nm}$, $\lambda_{\text{em}} = 470 \text{ nm}$). Treatment of **11** in a pH 7.4 buffered solution ($40 \mu\text{M}$) with the NO-releasing agent NOC-7 produced a change in emission intensity over 1 h at 410 and 470 nm by 1.17- and 0.75-fold, respectively.^{7,29} The NO detection limit for **11** is 100 nM .^{7,29} The fluorescence turn on of **11** by NO arises from dissociation of fluorescamine-PROXYL upon NO binding to the iron center, restoring the fluorescence of Mmc-cyclam (Scheme 4). Although **11** can monitor NO by fluorescence turn on at a physiological pH, it is not practical for the bioimaging of NO because of its sensitivity to O_2 , slow response to NO, and small fluorescence changes.

Diiron(II) Tetracarboxylate Complex. Several diiron(II) terphenylcarboxylate complexes with *N*-donor ligands have been reported.³⁰ We prepared a diiron(II)-based NO sensor $[\text{Fe}_2(\mu\text{-O}_2\text{CAr}^{\text{ToI}})_4(\text{Ds-pip})_2]$ (**12**, Figure 9) by an approach similar to that used for dicobalt(II) complexes **5** and **6**.¹⁹ Exposure of **12** (0.1 mM) to 1 equiv of NO in CH_2Cl_2 elicited a 4-fold fluorescence increase within 5 min ($\lambda_{\text{ex}} = 350 \text{ nm}$).¹⁹ The reaction of **12** with O_2 , however, also led to fluorescence enhancement by 2.8-fold over 15 min. IR studies of **12** (0.5 mM) with 10 equiv of NO revealed two new bands at 1797 and 1726 cm^{-1} , consistent with formation of an $\text{Fe}(\text{NO})_2$ unit, and concomitant loss of the carboxylate stretching band at 1605 cm^{-1} . These observations possibly indicate generation of a diiron tetranitrosyl complex with two bridging carboxylate ligands during the reaction.¹⁹ Thus, the NO-induced fluorescence increase would occur by ligand dissociation

from the diiron core. Although **12** reacts with NO resulting in a fluorescence increase, its O_2 sensitivity renders it unsuitable as a biological NO sensor.

Ruthenium(II) Tetraphenylporphyrins²³

Ruthenium(II) porphyrins form stable nitrosyl complexes upon exposure to NO.¹⁵ The axial positions on the Ru(II) center are available for fluorophore ligands as well. Ruthenium(II) porphyrins were therefore utilized to explore an additional route for sensing NO. We constructed ruthenium carbonyl tetraphenylporphyrin complexes with a dansyl-imidazole (Ds-im) or dansyl-thiomorpholine (Ds-tm) axial base, $[\text{Ru}(\text{TPP})(\text{CO})(\text{Ds-im})]$ (**13**) and $[\text{Ru}(\text{TPP})(\text{CO})(\text{Ds-tm})]$ (**14**) (Figure 10). These compounds were anticipated to detect NO via the fluorophore-displacement strategy.¹³

Reactions of **13** and **14** ($10 \mu\text{M}$) with 100 equiv of NO

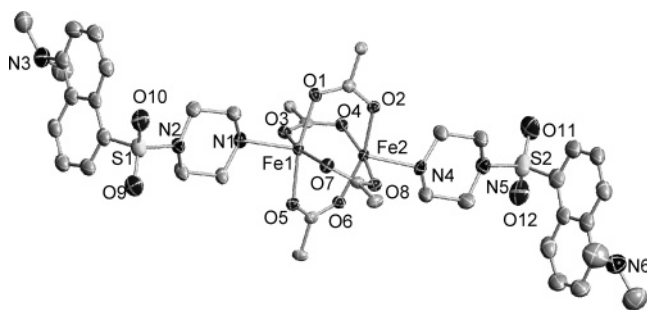


FIGURE 9. ORTEP diagram of **12** showing 50% probability thermal ellipsoids. The phenyl rings of $\text{Ar}^{\text{ToI}}\text{CO}_2^-$ ligands are omitted for clarity. The figure was taken from ref 21 with permission.

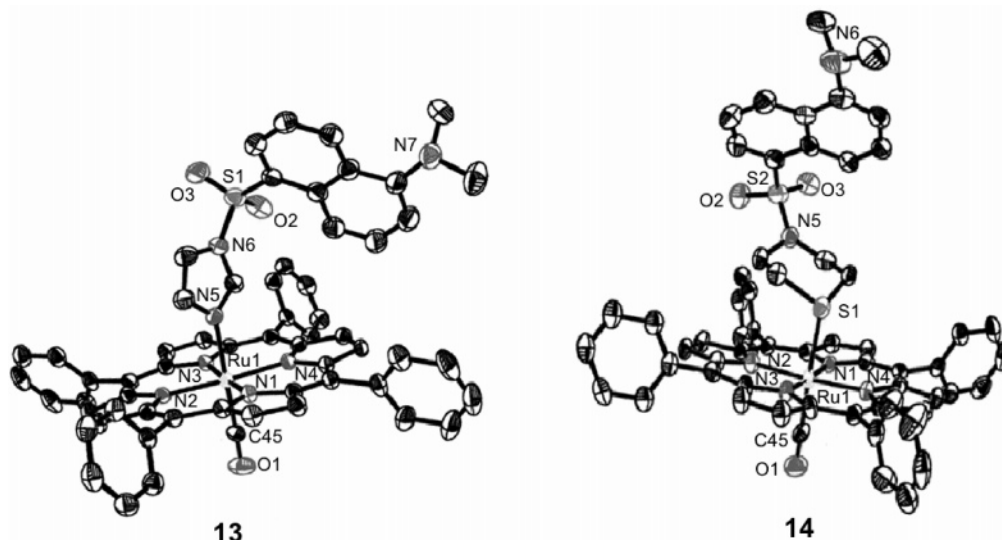


FIGURE 10. ORTEP diagrams of **13** and **14** showing 50% probability thermal ellipsoids. Reprinted with permission from ref 13. Copyright 2004 American Chemical Society.

in CH_2Cl_2 afforded a 19-fold increase in fluorescence within 20 min and an immediate 1.3-fold increase in fluorescence, respectively ($\lambda_{\text{ex}} = 368$ nm for Ds-im, $\lambda_{\text{ex}} = 345$ nm for Ds-tm). Isolation and characterization of the Ru-containing complex after reaction of **13** with NO revealed that both CO and the dansyl-containing fluorophore ligand dissociate during the reaction. The product isolated was $[\text{Ru}(\text{TPP})(\text{NO})(\text{ONO})]$.^{15,31,32} Release of the free fluorophore ligand from Ru(II) formed during the NO reaction of **13** was monitored by ^1H NMR spectroscopy.¹³ Thus, the fluorescence enhancement that occurs upon addition of NO to **13** and **14** arises from displacement of Ds-im or Ds-tm from the axial site, restoring their turn-on emission (Scheme 1.a).

Dirhodium(II) Tetracarboxylates as Reversible NO Sensors²³

Various ligands including NO can bind the axial positions of a tetrabridged dirhodium core.³³ A nitrosyl adduct obtained from the reaction of NO with solid $[\text{Rh}_2(\mu\text{-O}_2\text{-CMe}_4)]$ can be reversed upon heating to 120 °C,³⁴ suggesting that a dirhodium fluorophore complex might provide a reversible NO sensor. We designed dirhodium tetracarboxylate scaffolds containing bound fluorophores $[\text{Rh}_2(\mu\text{-O}_2\text{CMe}_4)(\text{Ds-pip})]$ (**15**) and $[\text{Rh}_2(\mu\text{-O}_2\text{CMe}_4)(\text{Ds-im})]$ (**16**) (Figure 11). These compounds were synthesized in situ by reaction of $[\text{Rh}_2(\mu\text{-O}_2\text{CMe}_4)]$ with Ds-pip and Ds-im.¹⁴ X-ray crystallographic studies of the isolated dirhodium tetracarboxylate complexes with Ds-pip and Ds-im revealed coordination to the axial positions of the dirhodium core by the piperazine and imidazole nitrogen atoms, respectively.¹⁴

When **15** was exposed to 100 equiv of NO in 1,2-dichloroethane (DCE) there was an immediate 26-fold increase in fluorescence ($\lambda_{\text{ex}} = 345$ nm).¹⁴ A 16-fold increased fluorescence was observed upon addition of 100 equiv of NO to a DCE solution of **16** ($\lambda_{\text{ex}} = 365$ nm).¹⁴ The

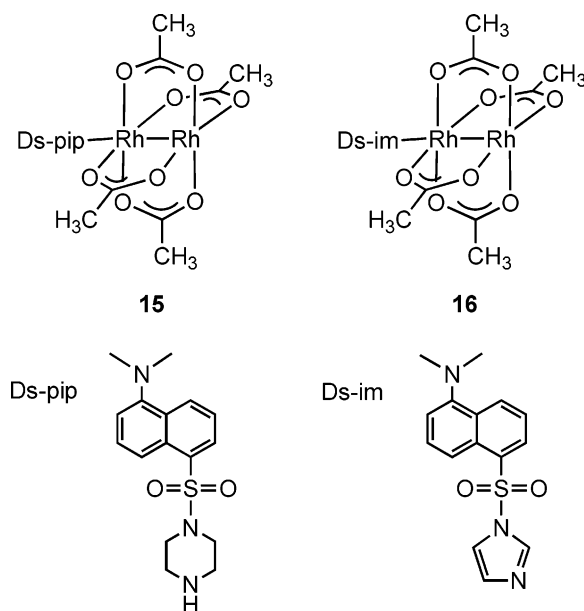


FIGURE 11. Chemical structures of **15** and **16**.

fluorescence response of both compounds was reversible, with a 4 μM lower detection limit for NO.¹⁴

NO sequentially generates mono- and dinitrosyl adducts with dirhodium tetracarboxylates. Although the mononitrosyl species has not been isolated, dirhodium dinitrosyl complexes were obtained and characterized by IR spectroscopy ($[\text{Rh}_2(\mu\text{-O}_2\text{CMe}_4)(\text{NO})_2]$, $\nu_{\text{NO}} = 1729$ and 1698 cm^{-1} in KBr, $\nu_{\text{NO}} = 1702$ cm^{-1} in DCE) and X-ray crystallography (Figure 12).¹⁴ Thus, the NO-induced fluorescence turn on is due to formation of metal nitrosyl species with concomitant dissociation of dansyl fluorophores from the Rh_2 core (Scheme 1.a).

A stopped-flow kinetic study of the reaction at -80 °C revealed it to be complete within the 1-ms mixing time of the instrument, corresponding to an on rate of $\geq 4 \times 10^6$ s^{-1} at 40 °C.¹⁴ Fast and reversible NO detection utilizing dirhodium complexes **15** and **16** suggests their potential value as real-time imaging agents for NO in biological

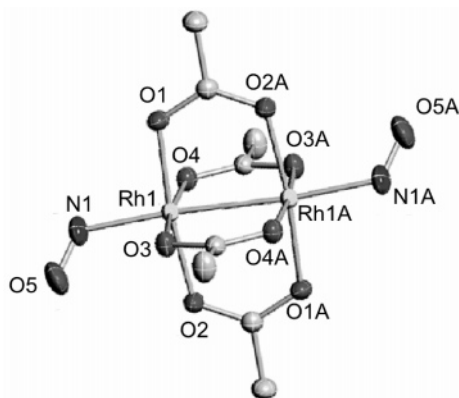


FIGURE 12. ORTEP diagram of $[\text{Rh}_2(\mu\text{-O}_2\text{CMe})_4(\text{NO})_2]$ showing 50% probability thermal ellipsoids. Reprinted with permission from ref 14. Copyright 2004 American Chemical Society.

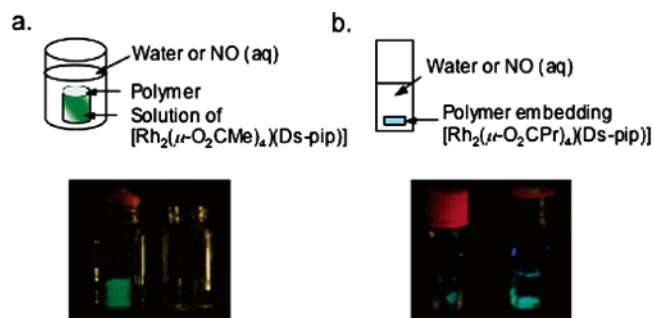


FIGURE 13. (a) Fluorescence response of a CH_2Cl_2 solution of **15** protected by a Silastic membrane against water in the outer vial (right) and upon introduction of 1.9 mM aqueous NO (aq) into the outer vial (left). Adapted with permission from ref 14. (b) Fluorescence response of Silastic membrane-embedded $[\text{Rh}_2(\mu\text{-O}_2\text{CPr})_4(\text{Ds-pip})]$ in water (left) and after exposure to a saturated NO aqueous solution (right).

systems. They are incompatible with aqueous media, however, since water itself can displace the fluorophore ligand and bind to the dirhodium core. One approach to achieving water compatibility is to isolate a solution of the dirhodium sensor behind a Silastic membrane that is impermeable to water but permits NO gas transport. In one such experiment the fluorescence of the CH_2Cl_2 solution of **15**, which was sequestered from a saturated aqueous NO solution by the membrane, immediately increased upon application of NO (Figure 13a).¹⁴ In a separate strategy the dirhodium sensor was embedded within the Silastic membrane. When membrane-encapsulated $[\text{Rh}_2(\mu\text{-O}_2\text{CPr})_4(\text{Ds-pip})]$ was treated with an aqueous solution of NO, an immediate fluorescence increase was observed (Figure 13b).³⁵ These experiments illustrate a potential approach to fabricating fiber-optic or film-based NO sensing devices for study in biological fluids using dirhodium-containing polymers.

Copper(II) Complexes²³

Copper(II) Dansyl Complexes. Quenching of the fluorescence of the luminescent ligand by coordination to a paramagnetic Cu(II) center can be restored by NO-induced reduction to a diamagnetic Cu(I) species (Scheme 1.b). We applied this strategy to develop two water-soluble

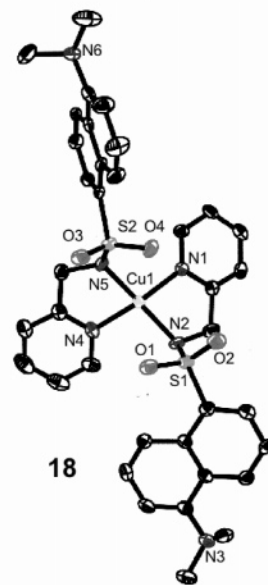
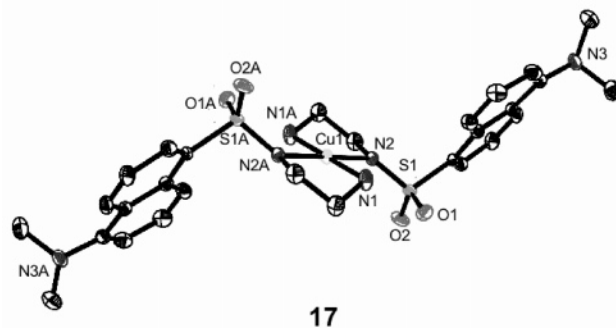


FIGURE 14. ORTEP diagrams of **17** and **18** showing 50% probability thermal ellipsoids. Reprinted with permission from ref 28. Copyright 2005 American Chemical Society.

Cu(II) complexes $[\text{Cu}(\text{Ds-en})_2]$ (**17**) and $[\text{Cu}(\text{Ds-AMP})_2]$ (**18**), where Ds-en and Ds-AMP are the conjugate bases of dansyl-ethylenediamine and dansyl-aminomethylpyridine, respectively.¹⁶ X-ray crystal structures of both **17** and **18** indicate that the Cu(II) center is coordinated by two dansyl-containing ligands (Figure 14).¹⁶

Fluorescence experiments demonstrated Cu(II)-induced quenching in both organic (4:1 $\text{CH}_3\text{OH}:\text{CH}_2\text{Cl}_2$) and buffered aqueous solutions, compared to the free ligands ($\lambda_{\text{ex}} = 342 \text{ nm}$).¹⁶ Upon addition of NO to an organic solution of **17** and **18** (20 μM , 4:1 $\text{CH}_3\text{OH}:\text{CH}_2\text{Cl}_2$), the emission intensity was immediately increased by 6.1-fold for **17** and 8.8-fold for **18** with a detection limit of $\geq 10 \text{ nM}$.¹⁶ Addition of NO to a buffered aqueous solution (50 mM CHES, pH 9.0, 100 mM KCl) of **17** or **18** (10 μM) also caused a fluorescence increase by 2.3- or 2.0-fold, respectively.¹⁶ Although this pH is not within the typical physiological range, these complexes allowed NO sensing for the first time in purely aqueous solutions with significant fluorescence turn on at physiologically relevant concentrations.

NO-induced fluorescence enhancement in these Cu(II) systems occurs by formation of a diamagnetic Cu(I) species, as mentioned previously, as well as dissociation of the sulfonamide functionality by protonation. Evidence

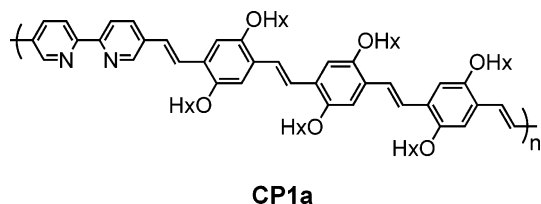


FIGURE 15. Chemical structure of CP1a.

that a Cu(I) species forms in NO reactions of the Cu(II) complexes was provided by EPR spectroscopy, which revealed a decrease in the Cu(II) EPR signal intensity.¹⁶ Protonation of the sulfonamide functionality was observed by IR spectroscopy ($\nu_{\text{N-H}} = 3083 \text{ cm}^{-1}$).¹⁶ A proton is generated from the reaction of ROH, either CH_3OH or H_2O , with a species with NO^+ character that is formed during the course of the reaction. Further support for the proposed mechanism was provided by studies of the reaction of NO in the absence of ROH and of ROH with NOBF_4 . The ^1H NMR spectrum indicated that complete dissociation of dansyl ligands does not occur after the NO reaction.¹⁶ Therefore, the fluorescence increase occurs by NO-induced reduction of Cu(II) to Cu(I) without complete dissociation of the ligand fluorophore from the Cu center (Scheme 1.b).

Copper(II)-Conjugated Polymer. A conjugated polymer (CP1a) composed of a bipyrindyl-substituted poly(*p*-phenylene vinylene) was prepared as a fluorophore ligand for Cu(II) (Figure 15).¹⁷ The fluorescence of CP1a was significantly quenched in the presence of Cu(II). Addition of NO to Cu(II)-CP1a (**19**) in 4:1 CH_2Cl_2 : $\text{CH}_3\text{CH}_2\text{OH}$ immediately induced a 2.8-fold fluorescence enhancement ($\lambda_{\text{ex}} = 462 \text{ nm}$, $\lambda_{\text{em}} = 542 \text{ nm}$).¹⁷ This fluorescence response is caused by reduction of Cu(II) to Cu(I) without fluorophore release (Scheme 1.b) as described above for **17** and **18**. Selectivity studies versus other reactive nitrogen species such as nitrosothiol (RSNO), NO^+ , and HNO, were performed and revealed that only nitroxyl elicited an immediate 2.8-fold increase in fluorescence.¹⁷ Thus, **19** is a turn-on fluorescence probe for both NO and HNO. The lower detection limit for NO by **19** is 6.3 nM.¹⁷

Copper(II) Anthracenyl-Cyclam. A copper(II) complex of a cyclam derivative having pendent anthracenyl groups, $\text{Cu}(\text{DAC})^{2+}$ (**20**) (DAC = bis(9-anthracylmethyl)cyclam), was recently reported (Figure 16).²¹ Addition of excess NO to weakly fluorescent **20** in aqueous CH_3OH (10:1 $\text{CH}_3\text{OH}:\text{H}_2\text{O}$) solution resulted in slow restoration of anthracene emission over 45 min.²¹ This increase in fluorescence occurs by release of the *N*-nitrosated DAC ligand from the Cu center with concomitant reduction of Cu(II) to Cu(I) (Scheme 1.c.ii). The presence of a Cu(I) species during the NO reaction was determined by optical spectroscopy (disappearance of a d-d absorption band at 566 nm) and electrochemical studies.²¹ Formation of the *N*-nitrosated DAC ligand during the reaction was confirmed by ESI-MS ($m/z = 610$ [DAC + NO]⁺) and ^1H COSY NMR spectroscopy (1:1 *E:Z* isomers).²¹ Ligand dissociation in the NO reaction of **20** may be explained by the less basic nature of the *N*-nitrosoamine and the

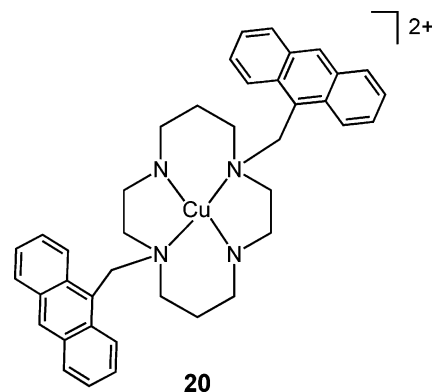
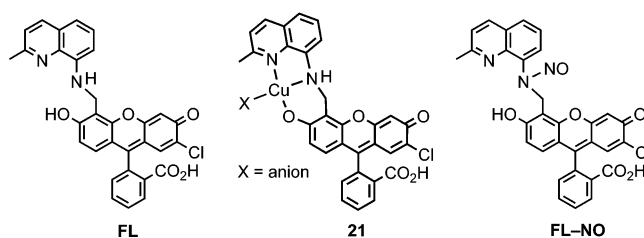
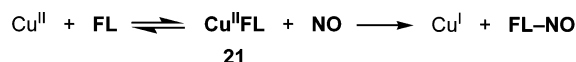


FIGURE 16. Chemical structure of **20**.

Scheme 5. NO Sensing by 21



geometric mismatch between the cyclam ring and Cu(I), which prefers a tetrahedral coordination environment.

Copper(II) Fluorescein Complex. For intracellular NO sensing we applied the strategy described in Scheme 1.c.ii to design a Cu(II) fluorescein complex. The Cu(II) fluorescein-based NO sensor CuFL (**21**) (FL = 2-{2-chloro-6-hydroxy-5-[(2-methyl-quinolin-8-ylamino)-methyl]-3-oxo-3*H*-xanthen-9-yl}benzoic acid) was formed in situ by reacting FL with CuCl_2 in a 1:1 ratio at pH 7.0 (50 mM PIPES, 100 mM KCl) (Scheme 5).²² Introduction of NO to **21** (1 μM CuCl_2 and 1 μM FL) at 37 °C led to an immediate 11-fold fluorescence enhancement, which continued to rise to 16-fold over 5 min with a sensitivity of 5 nM.²² Compound **21** is highly specific for NO over the biologically relevant species HNO, NO_2^- , NO_3^- , ONOO^- , H_2O_2 , O_2^- , and ClO^- .^{22,36}

NO-induced reduction of Cu(II) to Cu(I), forming the *N*-nitrosamine of FL (FL-NO), occurs in the NO reaction of **21** (Schemes 1.c.ii and 5). Reduction of Cu(II) to Cu(I) was confirmed by following the decrease of Cu(II) EPR signals.²² Formation of the *N*-nitrosated FL ligand was proved by product analysis using LC-MS and comparison with independently prepared FL-NO. The red-shifted UV-vis spectrum observed following addition of excess NO to **21** is the same as that of FL and different from the spectrum observed upon mixing FL with the Cu(I) salt $[\text{Cu}(\text{CH}_3\text{CN})_4](\text{BF}_4)$, indicating that FL-NO dissociates from the Cu center.²² Thus, the turn-on fluorescence is a result of *N*-nitrosated fluorophore displacement via reduction of the metal center (Scheme 1.c.ii).

The ability of **21** to detect NO directly, rapidly, and specifically at a physiological pH encouraged us to apply it to image NO in live cells. We tested **21** for its ability to

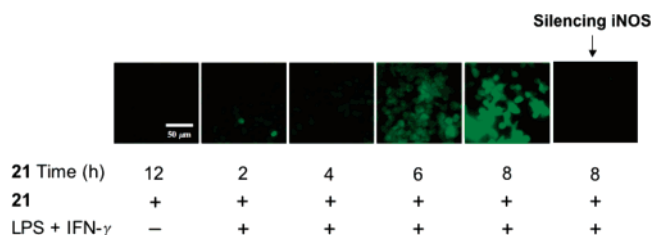


FIGURE 17. Detection by **21** of NO produced in Raw 264.7 cells activated by LPS and IFN- γ or in Raw 264.7 cells silenced with iNOS. Time depicted in the figure is the total incubation time of **21** with only cells or with cells pretreated with LPS and IFN- γ for 4 h.

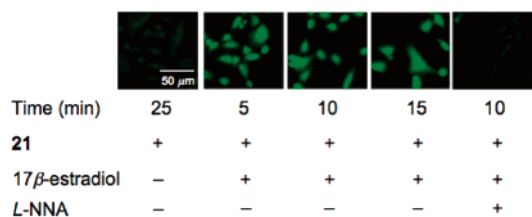


FIGURE 18. Detection by **21** of NO produced in SK-N-SH cells activated by 17 β -estradiol in the absence or presence of inhibitor (L-NNA). Time depicted in the figure is the total time of co-treatment of **21** and 17 β -estradiol.

visualize iNOS-generated NO in Raw 264.7 murine macrophage cells and cNOS-produced NO in SK-N-SH human neuroblastoma cells. Time-dependent NO generation in macrophage cells stimulated with bacterial lipopolysaccharide (LPS) and interferon- γ (IFN- γ) was monitored by **21** using fluorescence microscopy (Figure 17).²² The fluorescence intensity derived from **21** was diminished in macrophage cells in which iNOS was silenced by RNA interference (Figure 17) or in the presence of *N*^G-methyl-L-arginine (L-NMA), a known inhibitor of iNOS.²² These control experiments indicate that the observed results originate from the reaction of **21** with NO. Furthermore, the NO-induced fluorescence response, monitored after simultaneous administration of 17 β -estradiol and **21** to the neuroblastoma cells, was complete within 5 min (Figure 18).²² A diminished fluorescence response occurred in the presence of the cNOS inhibitor *N*^G-nitro-L-arginine (L-NNA) (Figure 18), confirming that NO generation is responsible for the fluorescence increase.²² Cytotoxicity assays of Raw 264.7 and SK-N-SH cells treated with **21** for 5 days demonstrated >80% cell survival, proving **21** to be nontoxic to live cells and suitable for bioimaging of NO.²²

Summary and Conclusion

Nitric oxide mediates beneficial and harmful biological events in the cardiovascular, immune, and nervous systems. Fluorescent probes have been developed for visualizing NO in biology. The commonly used organic molecule-based sensors are not capable of direct NO detection, a requirement for understanding fully the activity of nitric oxide in bioorganisms. Metal-based sensors are promising candidates for direct and specific NO detection, utilizing NO binding to the metal center. We and other groups have devised a variety of metal complexes described here as

fluorescent NO sensors. Cobalt(II) complexes (**1–10**), iron(II) complexes (**11** and **12**), ruthenium(II) porphyrins (**13** and **14**), and dirhodium(II) tetracarboxylates (**15** and **16**) clearly afford direct NO detection by fluorescence turn on through interaction of NO with the metal centers. NO chemistry at copper(II) centers also provides a valuable approach to fluorescence-based NO sensing (**17–21**). Very recently, the Cu(II) complex of a fluorescein-based ligand (**21**) has made NO detection at pH 7.0 and in live cells a reality. As summarized here, strategies for NO sensing by metal complexes include fluorophore displacement without metal reduction and metal reduction with or without fluorophore displacement. These approaches have facilitated novel probes for NO detection. Taken together, the metal complexes described here unequivocally demonstrate that fluorescent complexes of transition-metal ions are appropriate and practical for investigating the roles of NO itself in biology. We anticipate significant advances in this new area in the near future.

Work from our laboratory covered in this Account was supported by the National Science Foundation.

Note Added after ASAP Publication

There was an error in Scheme 1 in the version published ASAP October 4, 2006; Scheme 1 was replaced with the corrected version and published ASAP October 10, 2006.

References

- (1) Murad, F. Discovery of Some of the Biological Effects of Nitric Oxide and Its Role in Cell Signaling. *Angew. Chem., Int. Ed.* **1999**, *38*, 1856–1868.
- (2) Moncada, S.; Palmer, R. M. J.; Higgs, E. A. Nitric Oxide: Physiology, Pathophysiology, and Pharmacology. *Pharmacol. Rev.* **1991**, *43*, 109–142.
- (3) Conner, E. M.; Grisham, M. B. Nitric Oxide: Biochemistry, Physiology, and Pathophysiology. *Methods Enzymol.* **1995**, *7*, 3–13.
- (4) Lancaster, J. R., Jr. A Tutorial on the Diffusibility and Reactivity of Free Nitric Oxide. *Nitric Oxide: Biol. Chem.* **1997**, *1*, 18–30.
- (5) Wood, J.; Garthwaite, J. Models of the Diffusional Spread of Nitric Oxide: Implications for Neural Nitric Oxide Signalling and Its Pharmacological Properties. *Neuropharmacology* **1994**, *33*, 1235–1244.
- (6) Nagano, T.; Yoshimura, T. Bioimaging of Nitric Oxide. *Chem. Rev.* **2002**, *102*, 1235–1269 and references cited therein.
- (7) Hilderbrand, S. A.; Lim, M. H.; Lippard, S. J. In *Topics in Fluorescence Spectroscopy*; Geddes, C. D., Lakowicz, J. R., Eds.; Springer, 2005; pp 163–188 and references cited therein.
- (8) Hampl, V.; Walters, C. L.; Archer, S. L. In *Methods in Nitric Oxide Research*; Feelisch, M., Stamler, J. S., Eds.; John Wiley & Sons: New York, 1996; pp 309–318.
- (9) Malinski, T.; Mesaros, S.; Tomboulis, P. Nitric Oxide Measurement Using Electrochemical Methods. *Methods Enzymol.* **1996**, *268*, 58–69.
- (10) Katayama, Y.; Takahashi, S.; Maeda, M. Design, Synthesis and Characterization of a Novel Fluorescent Probe for Nitric Oxide (Nitrogen Monoxide). *Anal. Chim. Acta* **1998**, *365*, 159–167.
- (11) Soh, N.; Katayama, Y.; Maeda, M. A Fluorescent Probe for Monitoring Nitric Oxide Production Using a Novel Detection Concept. *Analyst* **2001**, *126*, 564–566.
- (12) Bergonzi, R.; Fabbrizzi, L.; Licchelli, M.; Mangano, C. Molecular Switches of Fluorescence Operating through Metal Centred Redox Couples. *Coord. Chem. Rev.* **1998**, *170*, 31–46.
- (13) Lim, M. H.; Lippard, S. J. Fluorescence-Based Nitric Oxide Detection by Ruthenium Porphyrin Fluorophore Complexes. *Inorg. Chem.* **2004**, *43*, 6366–6370.
- (14) Hilderbrand, S. A.; Lim, M. H.; Lippard, S. J. Dirhodium Tetracarboxylate Scaffolds as Reversible Fluorescence-Based Nitric Oxide Sensors. *J. Am. Chem. Soc.* **2004**, *126*, 4972–4978.

- (15) Ford, P. C.; Lorkovic, I. M. Mechanistic Aspects of the Reactions of Nitric Oxide with Transition-Metal Complexes. *Chem. Rev.* **2002**, *102*, 993–1017 and references cited therein.
- (16) Lim, M. H.; Lippard, S. J. Copper Complexes for Fluorescence-Based NO Detection in Aqueous Solution. *J. Am. Chem. Soc.* **2005**, *127*, 12170–12171.
- (17) Smith, R. C.; Tennyson, A. G.; Lim, M. H.; Lippard, S. J. Conjugated Polymer-Based Fluorescence Turn-On Sensor for Nitric Oxide. *Org. Lett.* **2005**, *7*, 3573–3575.
- (18) Franz, K. J.; Singh, N.; Spingler, B.; Lippard, S. J. Aminotroponimines as Ligands for Potential Metal-Based Nitric Oxide Sensors. *Inorg. Chem.* **2000**, *39*, 4081–4092.
- (19) Hilderbrand, S. A.; Lippard, S. J. Nitric Oxide Reactivity of Fluorophore Coordinated Carboxylate-Bridged Diiron(II) and Dicobalt(III) Complexes. *Inorg. Chem.* **2004**, *43*, 5294–5301.
- (20) Lee, J.; Chen, L.; West, A. H.; Richter-Addo, G. B. Interactions of Organic Nitroso Compounds with Metals. *Chem. Rev.* **2002**, *102*, 1019–1065.
- (21) Tsuge, K.; DeRosa, F.; Lim, M. D.; Ford, P. C. Intramolecular Reductive Nitrosylation: Reaction of Nitric Oxide and a Copper(II) Complex of a Cyclam Derivative with Pendant Luminescent Chromophores. *J. Am. Chem. Soc.* **2004**, *126*, 6564–6565.
- (22) Lim, M. H.; Xu, D.; Lippard, S. J. Visualization of Nitric Oxide in Living Cells by a Copper-Based Fluorescent Probe. *Nat. Chem. Biol.* **2006**, *2*, 375–380.
- (23) Fluorescence studies of metal complexes described in this Account were performed in the presence of excess (mM) NO. The concentrations of NO in vivo (picomolar to micromolar) are generally much lower.^{2,3,7}
- (24) Franz, K. J.; Doerrler, L. H.; Spingler, B.; Lippard, S. J. Pentacoordinate Cobalt(III) Thiolate and Nitrosyl Tropicoronand Compounds. *Inorg. Chem.* **2001**, *40*, 3774–3780.
- (25) Liu, Z.-H.; Duan, C.-Y.; Hu, J.; You, X.-Z. Design, Synthesis, and Crystal Structure of a *cis*-Configuration N₂S₂-Coordinated Palladium(II) Complex: Role of the Intra- and Intermolecular Aromatic-Ring Stacking Interaction. *Inorg. Chem.* **1999**, *38*, 1719–1724.
- (26) Lee, D.; Hung, P.-L.; Spingler, B.; Lippard, S. J. Sterically Hindered Carboxylate Ligands Support Water-Bridged Dimetallic Centers that Model Features of Metallohydrolase Active Sites. *Inorg. Chem.* **2002**, *41*, 521–531.
- (27) Lim, M. H.; Kuang, C.; Lippard, S. J. Nitric Oxide-Induced Fluorescence Enhancement by Displacement of Dansylated Ligands from Cobalt. *ChemBioChem* **2006**, web release date: June 21, 2006, DOI: 10.1002/cbic. 200600042.
- (28) Hilderbrand, S. A.; Lippard, S. J. Cobalt Chemistry with Mixed Aminotroponiminate Salicylaldehyde Ligands: Synthesis, Characterization, and Nitric Oxide Reactivity. *Inorg. Chem.* **2004**, *43*, 4674–4682.
- (29) Soh, N.; Imato, T.; Kawamura, K.; Maeda, M.; Katayama, Y. Ratiometric Direct Detection of Nitric Oxide Based on a Novel Signal-Switching Mechanism. *Chem. Commun.* **2002**, 2650–2651.
- (30) Yoon, S.; Lippard, S. J. Synthesis, Characterization, and Dioxygen Reactivity of Tetracarboxylate-Bridged Diiron(II) Complexes with Coordinated Substrates. *Inorg. Chem.* **2003**, *42*, 8606–8608.
- (31) Miranda, K. M.; Bu, X.; Lorkovic, I.; Ford, P. C. Synthesis and Structural Characterization of Several Ruthenium Porphyrin Nitrosyl Complexes. *Inorg. Chem.* **1997**, *36*, 4838–4848.
- (32) Kadish, K. M.; Adamian, V. A.; Van Caemelbecke, E.; Tan, Z.; Tagliatesta, P.; Bianco, P.; Boschi, T.; Yi, G.-B.; Khan, M. A.; Richter-Addo, G. B. Synthesis, Characterization, and Electrochemistry of Ruthenium Porphyrins Containing a Nitrosyl Axial Ligand. *Inorg. Chem.* **1996**, *35*, 1343–1348.
- (33) Boyar, E. B.; Robinson, S. D. Rhodium(II) Carboxylates. *Coord. Chem. Rev.* **1983**, *50*, 109–208.
- (34) Johnson, S. A.; Hunt, H. R.; Neumann, H. M. Preparation and Properties of Anhydrous Rhodium(II) Acetate and Some Adducts Thereof. *Inorg. Chem.* **1963**, *2*, 960–962.
- (35) Lim, M. H.; Lippard, S. J. Unpublished results, 2005.
- (36) Lim, M. H.; Wong, B. A.; Pitcock, W. H.; Mokshagundam, D.; Baik, M.-H.; Lippard, S. J. Direct Nitric Oxide Detection In Aqueous Solution by Copper(II) Fluorescein Complexes. *J. Am. Chem. Soc.* **2006**, in press.

AR950149T